Supplementary Information for Publication

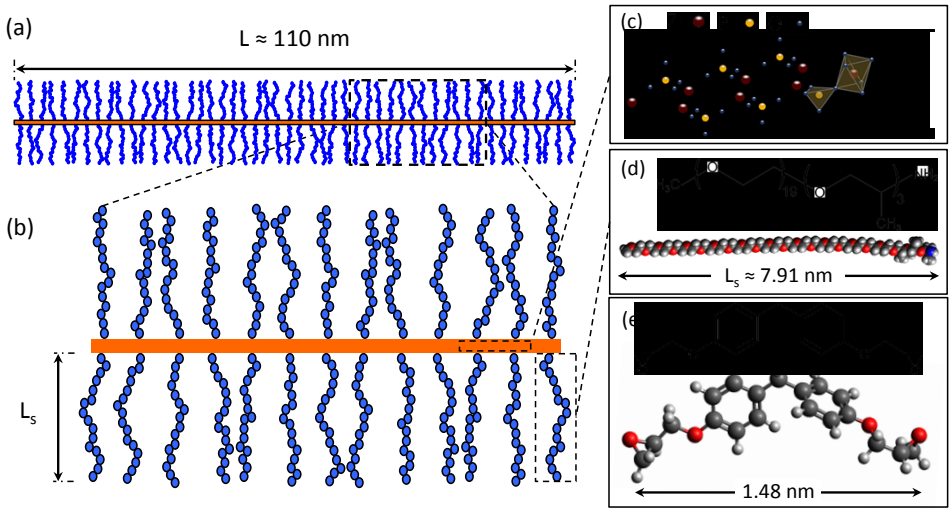

Figure S1. Schematic showing molecular-scale structure and dimensions of sterically-stabilized ZrP nanoplatelets and suspending medium used in this work. (a) Side profile of individual ZrP nanoplatelet with surface-attached oligomer brush. (b) Detail on section of ZrP showing relation between nanoplatelet thickness and length of extended oligomer. Distance between adjacent chains shown ~ 2x larger than expected to improve clarity. (c) Crystal structure of ZrP, adapted from Alberti and Constantino [1]. (d,e) Chemical structure and estimated dimensions of polyetheramine oligomer and DGEBF pre-polymer, respectively.

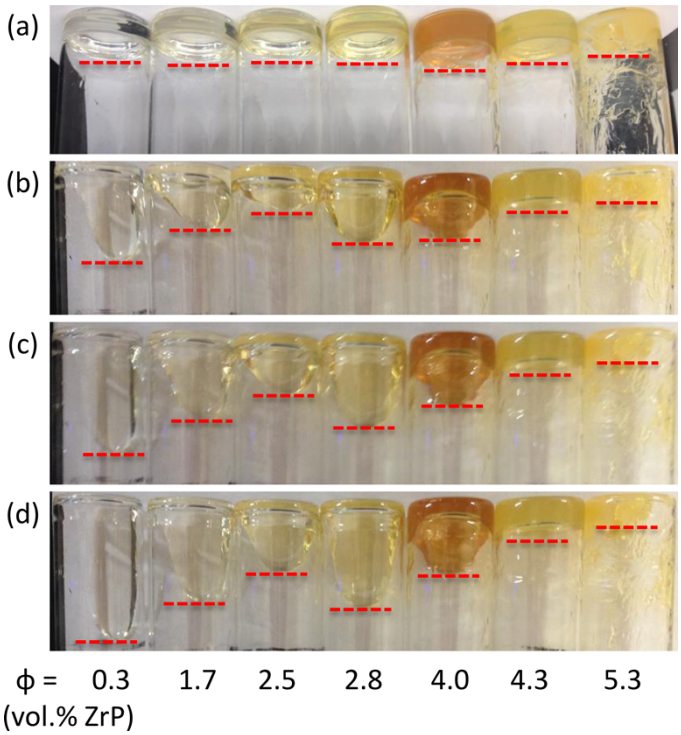

Figure S2. Photographs showing flow behavior of suspensions from Fig 1a. (a) Initial appearance of fluids before laying down on table. (b,c,d) Positions of fluids after laying flat on table for ~ 5, 10, and 30 sec, respectively. The concentration of the vials is in increasing order from the left, as indicated at the bottom of the figure. Some sample was removed from each vial to balance levels and allowed to equilibrate for one day. With the exception of the 5.3 vol.% suspension, which shows no change in appearance over several days, each fluid was able to fully recover its original shape after one day. The apparent time for recovery of shape followed observed trend in ability to flow inferred from photographs. To guide eye, dotted lines shown position of leading fluid edge at each time.

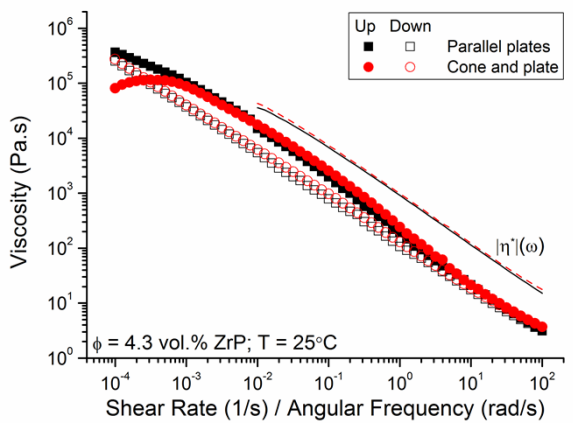

Figure S3. Flow curves for suspension containing 4.3 vol.% ZrP obtained using parallel plates (squares) and cone and plate (triangles) geometries. Filled and unfilled symbols correspond to step measurements obtained under conditions of increasing and decreasing shear rate, respectively. Magnitude of complex viscosity, |η*|, obtained from small-amplitude oscillatory measurements before and after shearing also included to show reproducibility of linear viscoelastic response, and breakdown in Cox-Merz behavior for "overlapped" suspensions. Measurements carried out at 25°C.

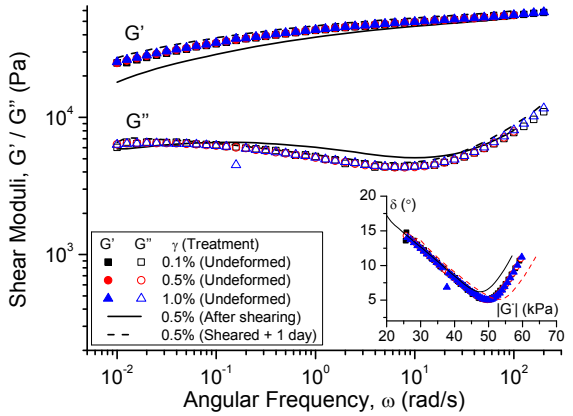

Figure S4. Linear viscoelastic response of smectic suspension containing 8.6 vol.% ZrP. Measurements carried out at three different strain amplitudes to verify linear viscoelasticity, and confirm stability of measurements over experimental time scale (~ 6 hr). Measurements carried out at T = 25°C with parallel plate fixtures.

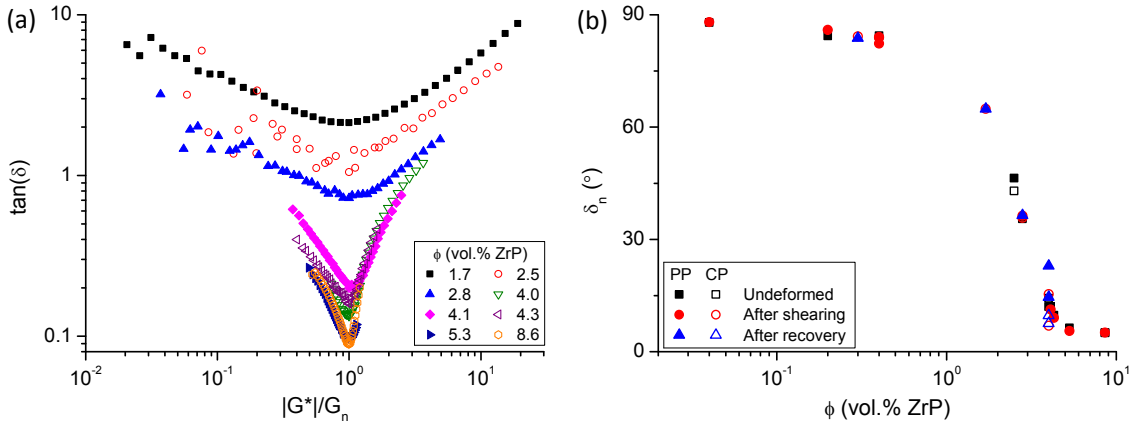

Figure S5. Summary of relaxation behavior for suspensions containing M1000-exfoliated ZrP nanoplatelets. (a) Loss factor, $\tan\delta = G^{''}/G^{'}$, plotted as function of reduced complex modulus, $G_r = |G^*|/G_{n,}$ for suspensions with smectic order. (b) Phase angle minima, δ_n, plotted as function of volume fraction for isotropic (ϕ = 0.04 – 0.4 vol.%) and smectic (ϕ = 1.7 – 8.6 vol.%) suspensions. Measurements carried out with parallel plate (PP, filled symbols) or cone and plate (CP, unfilled symbols) geometries on samples with different shearing histories. All measurements performed at 25°C.

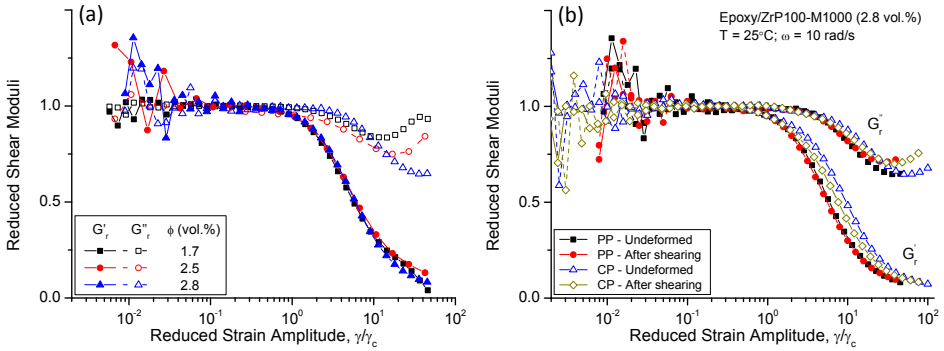

Figure S6. Representative curves showing non-linear viscoelastic response of less concentrated group of smectic suspensions. (a) Reduced shear moduli $G_r^{'} = G^{'}/G_o^{'}$ (filled symbols) and $G_r^{''} = G^{''}/G_o^{''}$ (unfilled symbols), as functions of reduced strain amplitude, γ/γ_c, for suspensions with ϕ = 1.7 (squares), 2.5 (circles), and 2.8 (triangles) vol.% ZrP. (b) LAOS of 2.8 vol.% suspension measured with parallel plate (filled symbols) and cone and plate (unfilled symbols) before and after shearing. Measurements carried out on undeformed samples at $\omega =$ 10 rad/s and T = 25°C with parallel plate fixtures.

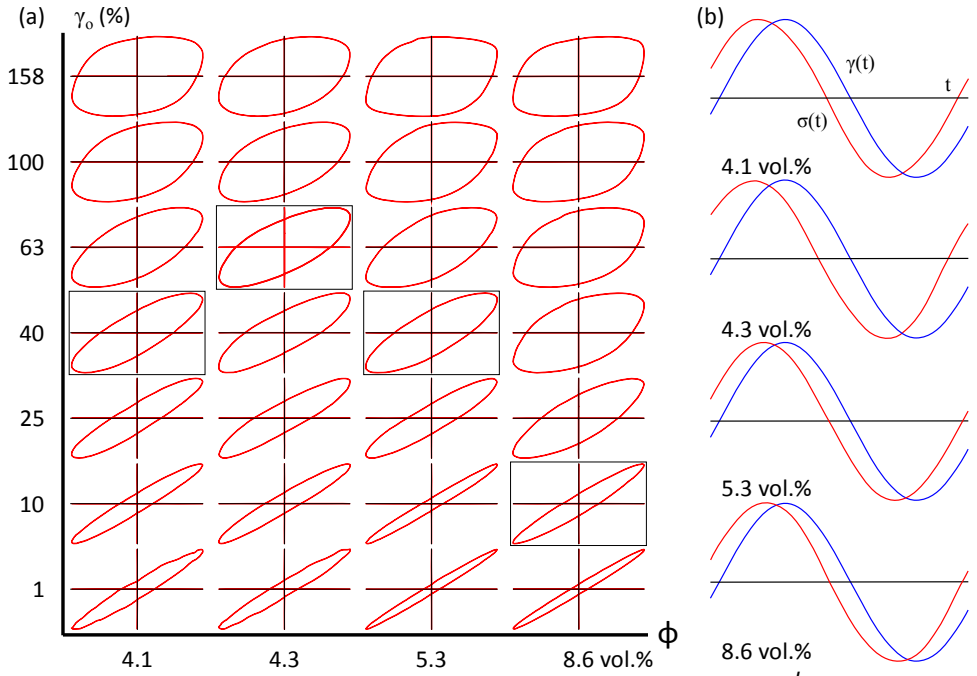

Figure S7. Raw LAOS data for concentrated suspensions of ZrP nanoplatelets with smectic order (ϕ = 4.1 – 8.6 vol.%). (a) Normalized Lissajous curves of stress, $\sigma(t)$ (y-axis), as function of strain, $\gamma(t)$ (x-axis). Curve for strain amplitude corresponding to maximum in $G^{''}$ shown with black border. (b) Raw waveforms (stress and strain as functions of time) for each suspension at $\gamma = \gamma_{max}$. At γ_{max}, the elliptical-shape of the Lissajous curves and sinusoidal stress signal both indicate that higher-order components of stress are not significant. Measurements carried out on undeformed samples at $\omega =$ 10 rad/s and T = 25°C with parallel plate fixtures.

Table S1. Mass and volume fraction of ZrP and oligomer phases for suspensions reported in this work.

System	c_{ZrP} [a] (wt.%)	c_{M1000} [b] (wt.%)	ϕ_{ZrP} [c] (vol.%)	ϕ_{M1000} [c] (vol.%)
ZrP-M1k-03	0.7	1.3	0.3	1.4
ZrP-M1k-17	4.0	7.4	1.7	8.2
ZrP-M1k-25	5.8	10.7	2.5	11.9
ZrP-M1k-28	6.3	11.5	2.8	12.9
ZrP-M1k-40	9.2	16.8	4.0	19.1
ZrP-M1k-41	9.4	17.3	4.1	19.6
ZrP-M1k-43	9.8	18.1	4.3	20.5
ZrP-M1k-53	12.0	22.0	5.3	25.3
ZrP-M1k-82	18.9	34.8	8.6	41.1

[a] Calculated using TGA based on residual mass of zirconium pyrophosphate after degradation at 900°C for 1 hr.
[b] Estimated from mass fraction of ZrP assuming stoichiometric ratio of 0.5:1 M1000:ZrP in final product.
[c] Calculated based on mass fraction of respective component using rule of mixtures equation $\phi_i = \left(c_i/\rho_i\right)/\sum_i \left(c_i/\rho_i\right)$ where c_i and ρ_i are the mass fraction and density of the *i*-th component in the suspension, respectively.

Table S2. Summary of d-spacing (in nm) for epoxy/ZrP-M1000 systems determined from SAXS measurements.

ϕ_{ZrP} (vol.%)	**Cured Film** [a]	ϕ_{ZrP} **(vol.%)**	**Uncured Liquid** [b]
2.1	24.2	1.7	32.2
2.9	15.3	2.5	22.6
3.2	15.7	2.8	18.5
4.4	5.9 6.4 [c]		
4.7	5.5 6.6 [c]	4.0	17.1
5.7	3.6 6.8 [c]	4.3	5.4
8.2	3.3 [d]	5.3	6

Volume fractions determined based on mass fraction measured using TGA. Spacing between layers of aligned nanoplatelets, d, calculated based on position of inner peak in scattering vector, q, using 1D paracrystal model (see Wong et al. [2] for additional details).
[a] Samples prepared by spray-coating solution of epoxy/ZrP in acetone on a glass substrate and evaporating solvent prior to full curing (Wong et al. [2]).
[b] Uncured epoxy fluids prepared by same method used in this work.
[c] Mean inter-layer distances estimated from electron micrograph images of cured films (Wong et al. [2]).
[d] Samples prepared by B-stage curing liquid (90 min at 110°C) and subsequently bar-coating on release paper using thin film applicator (Li et al. [3]). Bar-coated films fully cured prior to measurement.

References

1. G. Alberti and U. Costantino, *J. Mol. Catal.*, 1984, **27**, 235-250.
2. M. Wong, R. Ishige, K. L. White, P. Li, T. Higuchi, H. Jinnai, D. Kim, R. Krishnamoorti, A. Takahara, R. Nishimura and H.-J. Sue, *Nature Commun.*, 2014, **5**, 1-12.
3. P. Li, K. L. White, C. Lin, A. Muliana, D. Kim, R. Krishnamoorti, R. Nishimura and H.-J. Sue, *ACS Appl. Mater. Interf.*, 2014, **6**, 10188-10195.